Renewable Energy 179 (2021) 1472–1486

Contents lists available at ScienceDirect

Renewable Energy

journal homepage: www.elsevier.com/locate/renene

Novel wind resource assessment and demand flexibility analysis for community resilience: A remote microgrid case study

Chong Her [a], Daniel J. Sambor [b], Erin Whitney [a, *], Richard Wies [c]

[a] Alaska Center for Energy and Power (ACEP), University of Alaska Fairbanks, PO Box 755910, Fairbanks, AK, 99775-5910, USA
[b] Department of Civil and Environmental Engineering, Stanford University, Stanford, CA, 94305, USA
[c] Department Chair, Electrical and Computer Engineering Department College of Engineering and Mines, University of Alaska Fairbanks, PO Box 755915, Fairbanks, AK, 99775-5915, USA

ARTICLE INFO

Article history:
Received 2 March 2021
Received in revised form
21 June 2021
Accepted 21 July 2021
Available online 22 July 2021

Keywords:
Wind assessment
Microgrid
Arctic region
Dispatchable loads
Food-energy-water systems

ABSTRACT

With the increasing effects of climate change and high costs of energy, many rural Alaska communities are working to implement local alternative energy solutions to improve energy security. Integrating renewable energy systems can reduce reliance on fossil fuels and subsequently improve food, energy, and water (FEW) security. In this study, wind energy modeling techniques using local airport meteorological data were convolved with community loads to determine the most cost-effective combinations of wind turbine technology and dispatchable loads for improving FEW security in a southwestern Alaska village. This approach is different from wind assessments that exclusively analyze wind resources. A 100 kW wind turbine was determined to be suitable for the community, resulting in a capacity factor of 16.7% and levelized cost of energy (LCOE) of $1.15/kWh, with diminishing returns for higher wind turbine capacity. The results from the dispatchability study indicated that dispatchable loads could handle the intermittency of the wind resource with up to 86% of their annual load met. More work is needed to understand the impact of integrating and scheduling dispatchable loads into the grid in practice.

1. Introduction

With decreasing costs of renewable energy technologies along with volatile oil prices, renewable energy has become an appealing option in many rural communities [1]. This trend is especially true in Alaska's several hundred remote communities, where subsistence hunting, food production, industry, and household and municipal functions all depend primarily on expensive imported diesel and gasoline. As a result, communities are vulnerable to economic, environmental, or social changes that affect fuel prices [1,2].

Food, energy, and water security are inextricably linked in rural Alaska. High fuel prices result in exorbitant electricity costs, exceeding $1/kWh in some communities before subsidies [3,4]. Diesel fuel is shipped by plane or barge in short seasonal windows and then typically combusted in powerhouse generators that are maintained by each community. Since any food beyond what is harvested locally is also imported, food and fuel prices are tightly coupled. Climate change exacerbates these circumstances, as hunting and gathering routes are compromised by melting permafrost and ice [5]. Often, residents must decide between spending money on food or fuel to heat their homes [6,7]. Food grown in local greenhouses is one solution to reduce imports, yet there remains a substantial need for energy to operate the greenhouses in cold and dark seasons. Similarly, water can be expensive to process using electricity from diesel generators, often resulting in low water consumption per capita and increased risk of disease from contaminated water or poor sanitation.

Wind resources represent a viable energy alternative in many Alaska communities. As wind turbine technology has matured and become more affordable, interest in small-scale wind turbine installations has grown in western Alaska. To maximize the effectiveness of wind turbines, it is essential to identify installation locations with the greatest wind resources [8]. However, rural communities often lack data acquisition infrastructure, and their remoteness limits opportunities for detailed site surveys [9,10]. Due to the varied terrain in many of these communities, specific wind flow modeling is ideal for obtaining accurate data, but this requires techniques that are often computationally intensive [10].

* Corresponding author. Alaska Center for Energy and Power University of Alaska Fairbanks, PO Box 755910, Fairbanks, AK, 997775-5910, USA.
E-mail address: erin.whitney@alaska.edu (E. Whitney).

https://doi.org/10.1016/j.renene.2021.07.099

Global databases or mesoscale modeling and national or regional wind atlas data have been used to model wind resources [11–13]. However, the heights of consideration (50, 80, and 100 m above ground) and low resolution (1 km) pose challenges. This information is useful for understanding wind patterns and broad development areas, but it cannot account for issues caused by complex terrain [10]. Given these circumstances, local meteorological data from airports may be the best option.

However, no comprehensive model has been developed that is broadly applicable to Arctic communities—a model that can translate local wind resource data into potential energy, integrate community desires for type and size of wind turbine(s), and make accommodations for loads that may be installed to absorb excess energy. Thus, the purpose of this analysis is to combine wind modeling techniques using local airport meteorological data and convolutional load integration to determine the most cost-effective combination of wind turbine technology and loads that can improve food-energy-water security in a southwestern Alaska village. The community of interest has a population of about 70 people with 25 housing units and three 67 kW diesel-electric generators as the primary source for energy generation [14]. The community has recently installed an in-river hydrokinetic power generation device and has expressed interest in wind turbine technology, as well as modular and dispatchable loads to improve food and water security [15].

Loads that can be controlled to operate on demand with variable renewable energy supply are termed dispatchable loads. Dispatchable loads that also improve food and water security are particularly useful for Arctic communities. The dispatchable loads of interest in this study include a CropBox© container farm for growing food indoors year-round, a Lifewater™ system for treating residential sewage, a Water Reuse system for recycling greywater, and a residential water heater. These choices of dispatchable loads are by no means exhaustive but represent possible and realistic additions to remote community infrastructure in Alaska.

This analysis is part of the larger National Science Foundation “MicroFEWs” project examining the connection between renewable energy and the Food-Energy-Water (FEW) nexus in remote cold-region communities [15]. One key insight is that communities can create synergies by selecting wind turbines and modular food-water technologies as part of the same modeling process, which can create cost savings and further improve FEW security. For example, instead of choosing a wind turbine coupled with a battery to store excess energy, the excess energy generation can be matched with demand profiles of specific loads directly such that a smaller battery, or no battery, is needed. In general, the FEW nexus concept can orient community decision-makers toward optimizing the integration of various local renewable technologies with food-water loads to manage trade-offs and achieve sustainable development goals [9,16–18].

Overall, this study aims to determine how communities can increase their use of wind energy and redirect excess energy by evaluating the best match between specific wind turbines and dispatchable loads. An objective of the study is to develop a tool that remote communities can use for assessment of the wind resource. Dispatchability analysis derives from the necessity of using innovative approaches for integration of renewable energy in remote communities. The methods of assessment are discussed in Section 2, which details the wind resource data and modeling techniques to determine the amount of excess wind energy generation in comparison to the current community load. A convolutional integration model is presented in Sec. 2.4 to match selected wind turbines (Sec. 2.5) with specific dispatchable loads (Sec. 2.6). Results of each wind turbine's generation profile, the cost-effectiveness of each scenario, and the optimal integration with dispatchable loads are presented in Sections 3.1, 3.2, and 3.3, respectively.

2. Methods

Fig. 1 shows a flow diagram of the wind resource assessment, wind turbine selection process, cost analysis, and dispatchability analysis processes used in this study. Three different criteria were utilized to test and verify wind resource data before subsequent evaluations were carried out: 1) measured parameter checks, 2) data recovery rate, and 3) sufficient comparison checks. The measured parameter checks and data recovery rate determined if the model passed the data verification tests. The sufficient comparison criteria compares the wind analysis results to those produced with Windographer©, a commercially available software. The availability and temperature criteria ensured that the wind turbine was both commercially available and could operate in the Alaska environment. The capacity factors of the selected wind turbines were then compared with known historical wind project capacity factor ranges and used to generate the cost per installed wind capacity and levelized cost of energy (LCOE) estimates. Based on the capacity factor, cost per installed capacity, and LCOE estimates, the best suitable wind turbine was selected. Finally, the convolution between the excess energy with the selected wind turbine and different dispatchable loads was carried out to evaluate feasibility and usefulness.

2.1. Data collection and processing

Wind speed data were collected from the community's local airport meteorological station. Hourly meteorological data from January 1, 2015 to December 31, 2019 at a 10-m height were obtained through the Automated Surface Observing System (ASOS) Network from Iowa State University (Iowa Environmental Mesonet) [19,20]. A sample year of wind speed data is shown in Fig. 2. The annual mean wind speed was about 4 m/s with a wind power density of about 110 W/m^2.

The data verification guidelines of the National Renewable Energy Laboratory (NREL) and the International Renewable Energy Agency (IRENA) were followed to validate the data from the meteorological station [21,22]. The data were down sampled into hourly time steps, then validated using general system completeness checks and measured parameter checks, treatment of suspect and missing data, and data recovery rates [22]. Measured parameter checks consisted of range tests (allowable upper and lower limits) and trend tests (change over time). The dataset exhibited some missing values, though the data recovery percentage still exceeded 90% as a criterion for continued analysis [21,22].

Community electric load demand profiles were obtained from the local utility. The files were combined into a single year load demand profile by averaging the loads by date and time annually then aggregated to hourly temporal resolution. The community's annual energy demand was 297.6 MWh with an average annual load demand of 40.3 kW.

2.2. Wind resource assessment

The wind resource assessment was carried out using standard wind assessment methods and was programmed in Python to analyze wind data by determining the annual mean wind speed, standard deviation, Weibull distribution, histogram, wind power density, and wind rose [22–27]. Please see Appendix A for equations used for the wind resource assessment calculations. With

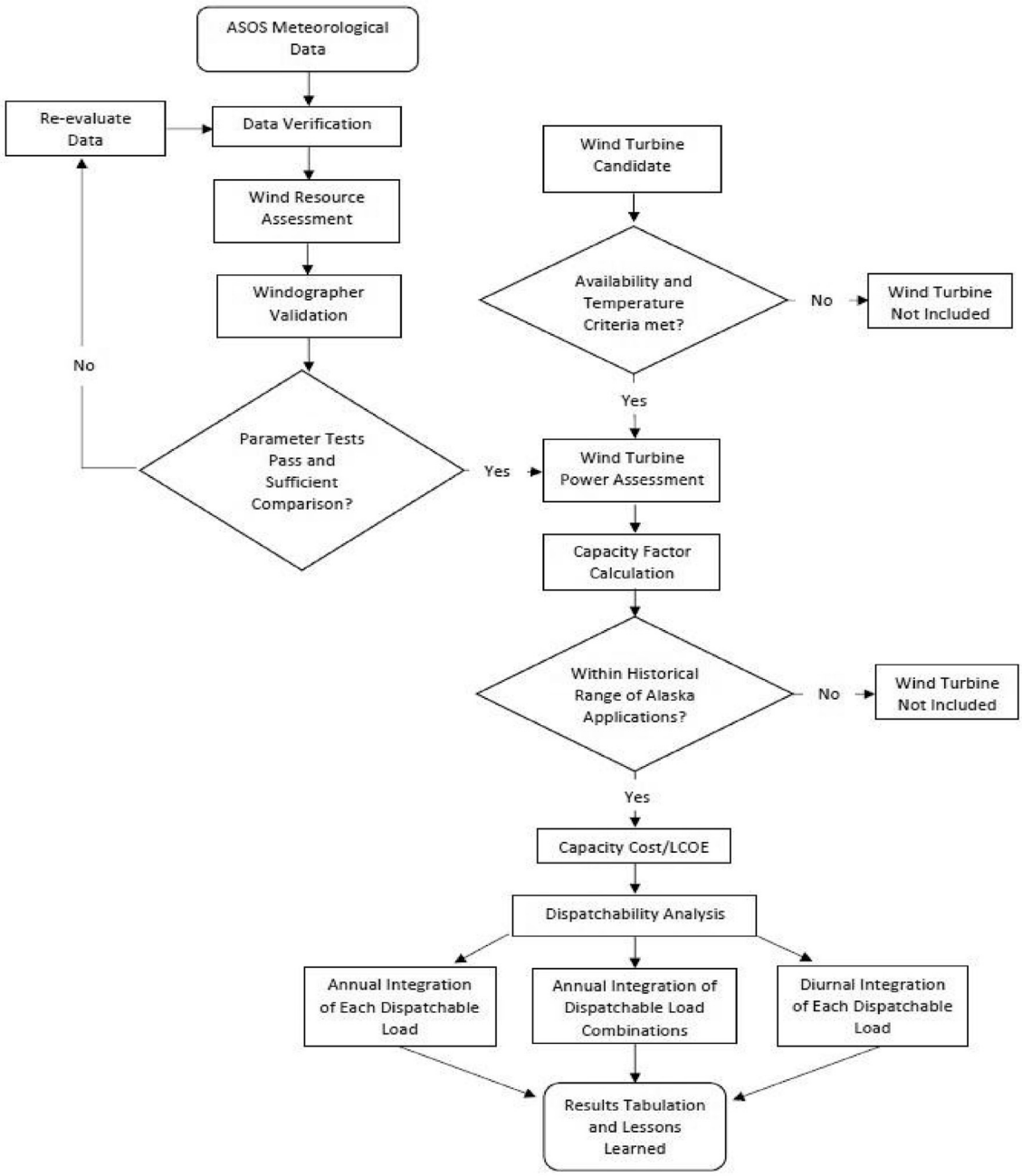

Fig. 1. A flow diagram of the analysis methods and criteria, including wind resource assessment, wind turbine selection, cost analysis, and dispatchability analysis processes.

Windographer© software, the results of the programmed assessment process were validated. Table 1 displays the comparison of data recovery (DR), annual mean wind speed, minimum and maximum wind speed, wind speed standard deviation, and wind power density using both Windographer© and the programmed assessment process. The validation process was conducted with raw data without excluding error values. Another assessment was conducted with the exclusion of errors, recurring zero values, and is also presented in Table 1.

The results in Table 1 demonstrate that the Python wind resource assessment model and Windographer© produced similar results. As shown in Fig. 3, this agreement was also true for wind rose generation. The wind roses illustrate that the prevailing wind directions are northeast and south, with northeast being dominant.

2.3. Wind turbine power assessment

Twenty-four wind turbine candidates with capacities between 50 kW and 900 kW were selected based on case studies by the Alaska Energy Authority (AEA), V3 Energy LLC reports, and others (see Appendix B) [28–31]. Wind turbines were evaluated for their commercial availability and their operating suitability in an environment where temperatures can range from −50 °C to 35 °C. Individual wind turbine specifications were obtained from manufacturer websites or the wind-turbine-model database [32–34]. Wind turbine power curves as a function of wind speed were interpolated into power values at 1 m/s increments. Then, 0.25 m/s-increment power curves were generated using polynomial fits, with R^2 values for the fit between the model and manufacturer curves of >0.999.

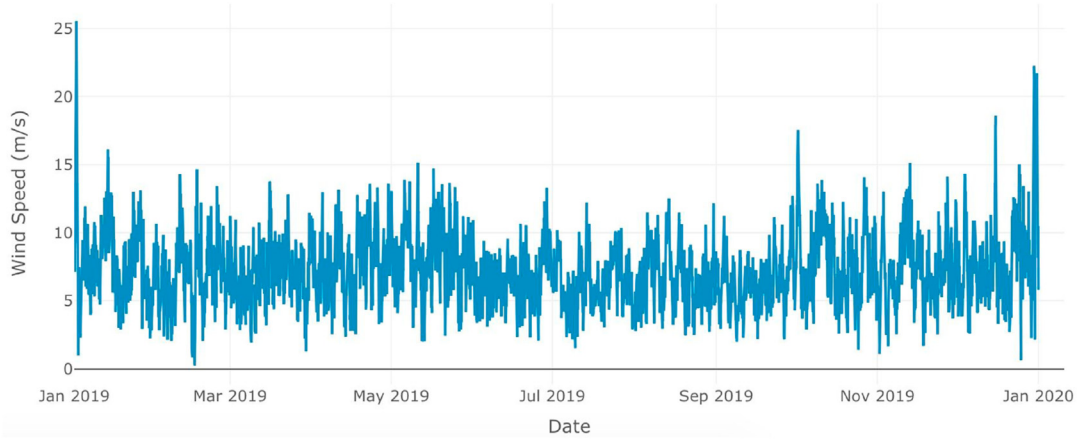

Fig. 2. Average hourly wind speed (m/s) January 1 to December 31 with an annual mean wind speed of about 4.0 m/s. Wind speeds were generally higher in winter and spring.

Table 1
Comparison of Windographer and programmed techniques.

	Windographer	Python Model w/o exclusion	Python Model w/exclusion
	Wind Speed (m/s)		
Height (m)	10	10	10
Possible Data Points	43800	43800	43800
Recovered Data Points	40911	40911	40265
Data Recovery (DR)	93.40%	93.40%	91.29%
Annual Mean	4.002	4.002	4.006
Minimum	0	0	0
Maximum	24.179	24.179	24.179
Std. Dev	2.77	2.77	2.74
	Weibull Distribution Parameters		
Scale factor (A) (m/s)	4.423	4.402	4.473
Shape factor (k)	1.471	1.491	1.535
	Wind Power Density		
Annual Wind Power Density (W/m^2)	113.00	109.61	109.12

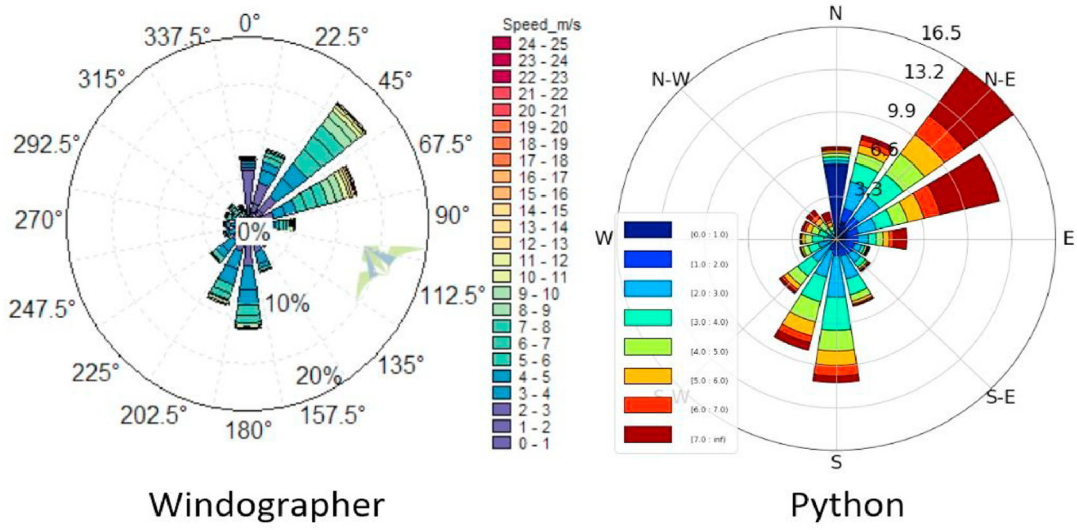

Fig. 3. Wind rose comparison of Windographer (left) and programmed techniques using Python (right) with 1 m/s increment increase.

Hourly wind power production was generated using wind speeds extrapolated at the hub height of a selected wind turbine using the power law. It should be noted that the wind power law only applies to flat terrain; in complex terrain, on-site measurements are needed. While most rural Alaska communities are surrounded by complex terrain, it was assumed that the community terrain was flat (wood plain) with a roughness coefficient of 0.24 m [22].

2.4. Capacity factor

The capacity factor is the ratio of the actual wind energy absorbed by the grid and the wind energy that could be produced if

operating at rated capacity throughout a given period [31]. The time series capacity factor was calculated based on the annual hourly wind power production and load demand, taking into consideration the technical minimum load of the generators (30%) and maximum instantaneous wind supply, assumed to be 50% of the instantaneous load demand, given no energy storage or dispatchable loads to maintain grid stability [31,35]. The community's diesel powerhouse consists of three 67 kW generators, and thus each generator must operate at a minimum of 20 kW. Any unabsorbed wind generation or diesel generation above the community load profile is considered excess generation.

The results from the time series capacity factor calculation were compared with the results from the probabilistic methods, which considered the probability of occurrence for every possible scenario in the convolution of the wind power production scenarios (N) and load demand scenarios (M) [35]. The ranges of both probabilities were generated between the *Minimum* (P_{min}) and *Maximum* (P_{max}) wind power in each hour and hourly load demand values with power increments (kW) calculated using Equation (1). The different wind power production scenarios (P_{wj}) are the aggregate of the energy increments generated with range N. The probability of occurrence of the wind power production is ($g(P_{Wj})$, j = 1, N), corresponding to the probability distribution of the scenarios in the range N calculated using Equation (1) [35].

$$Power\ \ Increment = \frac{P_{max} - P_{min}}{Number\ \ of\ \ probabilities\ \ under\ \ consideration(M\ or\ N)} \quad \text{Eq. 1}$$

The load demand (P_{Li}) was considered in a hourly annual duration (h_i), and the corresponding probability of occurrence is ($f(P_{Li}) = h_i/8760,\ i = 1,\ M$). The convolution of the wind power production probability ($g(P_{Wj})$) and load demand probability ($(f(P_{Li}))$) results in a two-dimensional matrix MxN using Equation (2) [35]. The values in this matrix correspond to the probability of occurrence of the two scenarios at the same time, as shown in Fig. 4.

$$\Pi ij(P_{Li,}P_{Wj}) = f(P_{Li})\ g(P_{Wj}),\ \{i = 1,\ M,\ j = 1,\ N\} \quad \text{Eq. 2}$$

A key assumption was that the maximum wind absorption capacity was based on the diesel generator minimum loading in all scenarios until the electric demand is met or exceeds the diesel generator capacity. The maximum allowable wind absorption was calculated based on the technical minimum of operating the diesel generators and the community load demand in each scenario; this was compared with wind power production scenarios to ensure no generation exceeded the maximum absorption limit. The scenarios were summed to determine the total wind energy absorbed and total excess energy (available for use in dispatchable loads) over the course of a year.

This probabilistic method is more precise in estimating the total absorption of wind power generation compared to the time series method; thus, this is a more accurate method of calculating capacity factors. This increase in precision comes about because the probabilistic method considers the probability of occurrences of each scenario whereas the time series method involves a direct hourly comparison of the power production and load demand. The accuracy of the time series method can be improved with the utilization of power curves that have smaller wind speed increments. For example, as the power curve wind speed increment decreases from 1 m/s to 0.25 m/s, the production becomes more accurate. If this increment is reduced further, the total wind power generation will be closer to that of the probability method. Although there is a mismatch, the percent difference is minimal and therefore can be considered adequate.

2.5. Wind turbine economics in Alaska

The capacity costs ($/kW) of installing the selected wind turbines, and resulting levelized cost of energy (LCOE, $/kWh), were determined based on data from 103 wind projects in Alaska with a

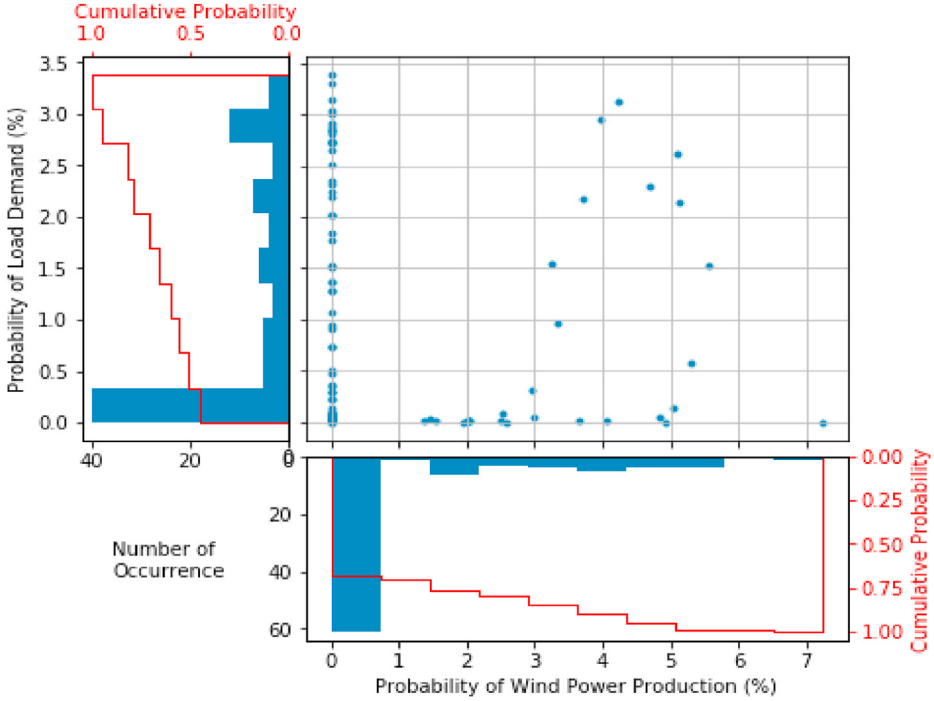

Fig. 4. Convolution of probability of load demand (left) and probability of wind power production (bottom) plotted as histograms. Each point in the scatter plot illustrates the possibility of occurrence of each scenario from both probabilities. The possibility of occurrence is used to calculate the wind power that can be absorbed by the power grid.

capacity range of 50–5000 kW between 2008 and 2016 [36]. The LCOE was calculated with the assumption of $0.036/kWh for yearly operation and maintenance costs with an increasing inflation rate of 2%, an interest rate of 5%, and a 20-year lifetime [36]. For this study's purpose, the LCOE for each installed capacity was extrapolated for a 5–10% capacity factor, from the 20–40% capacity factor range, using a second-order polynomial curve fit of existing data and resulting R^2 values of 1. The cost per installed capacity and LCOE tables values used in this cost analysis can be found in Appendix C.

2.6. Dispatchability

Dispatchable loads are defined as components of the community electric demand profile that can be controlled to turn on and off or flexibly operate along a spectrum of power demands. In this analysis, these loads are assumed to operate based on historical data of their operation to understand how much excess generation they can absorb with no controls as a conservative case. Then each of the loads can be analyzed for the best match with wind generation to inform communities on which may be most suitable for installation and future control in practice. This determination was conducted by convoluting the excess power production profiles with a dispatchable load's demand profile over a year to determine the total excess energy that could be absorbed. This convolution process was the same as that described in Section 2.4. For each hour of the year, the ratio of excess energy to the demand of the four dispatchable loads was also calculated as a metric to evaluate the best match between wind turbines and dispatchable loads.

The analysis first considered adding one type of dispatchable load (Sec. 3.3.1) and then a combination of dispatchable loads (Sec. 3.3.2) at every housing unit. When a type of dispatchable load was chosen, its load profile (based on typical historical operation, as shown in Fig. 5) was convoluted with the excess power production profile. The purpose of this analysis was to determine how much of the dispatchable load demand would be met by wind. In reality, the balance of dispatchable load demand would be met by diesel generation to ensure that the loads satisfy FEW security (such that plants do not die in a container farm if the wind stops, for example). However, diesel generation was not modeled in this analysis.

The integration of dispatchable loads was first considered in aggregation over a year (Sec 3.3.1 and Sec 3.3.2), and then modeled on an hourly basis (Sec. 3.3.3) for finer time-scale analysis of excess energy utilization. The objective of this approach was to provide a simple tool for recommending a type of dispatchable load for consideration by the community, assuming no alteration or control of its typical demand profile. Further optimization of the dispatchable load operation profile relative to excess wind energy was out of the scope of this work and has been analyzed previously in the literature with more computationally-intensive models [37].

This study considered the addition of four types of dispatchable loads that simultaneously benefit food and water security. The four dispatchable electric loads included a CropBox© container farm, a Lifewater™ modular sewage treatment unit, a household Water Reuse system, and a standard residential electric water heater. These loads were chosen based on preferences of the community. The power capacities of each dispatchable load are shown in Table 2.

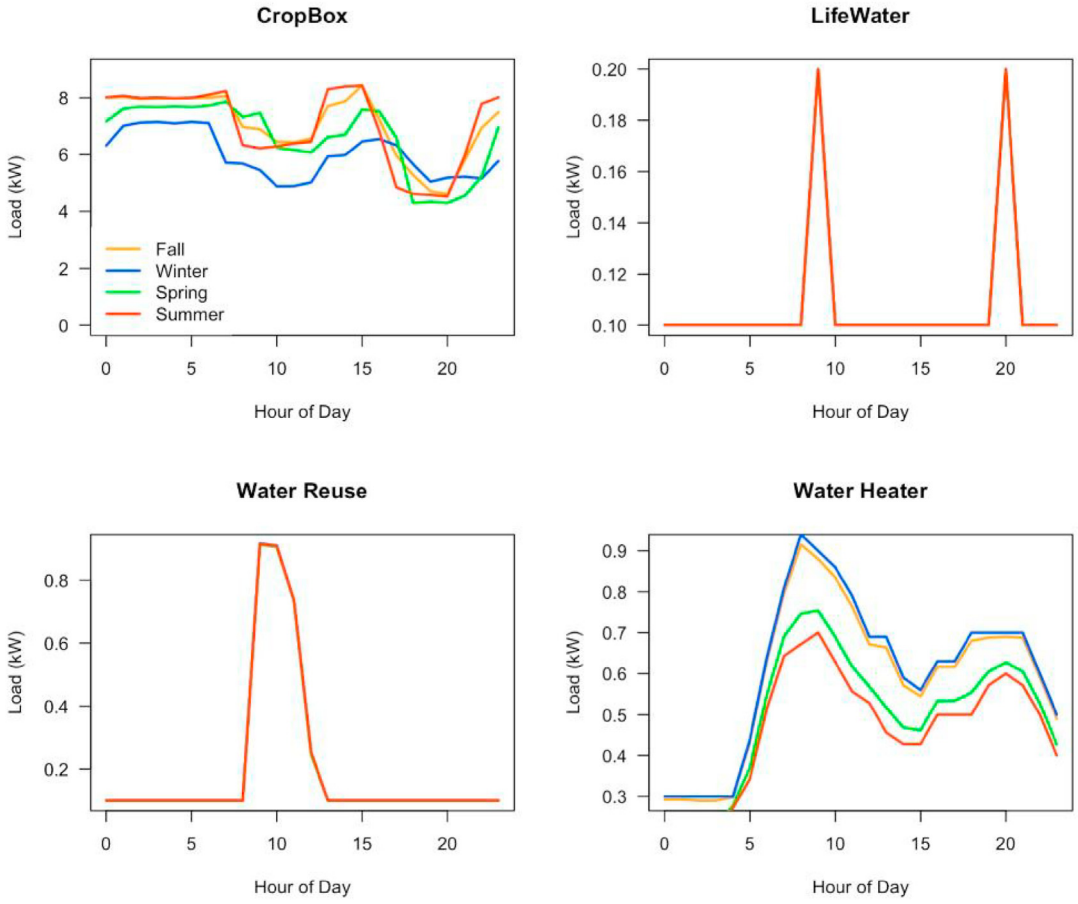

Fig. 5. Average seasonal load profiles of one unit of each dispatchable load. Note that the Water Reuse and Lifewater™ demand profiles are modeled based on the same behavior in each season.

Table 2
Dispatchable load power characteristics for four dispatchable systems.

	CropBox©	Lifewater™	Water Reuse	Water Heater
Average Power (kW)	6.6	0.11	0.2	0.54
Peak Power (kW)	8	0.2	1	1

A container farm, such as a CropBox© system, allows for growing herbs and greens in an indoor hydroponic system year-round to supplement food imports and subsistence hunting and gathering. Prior and current analysis using data from a CropBox© in Whitehorse, Yukon, Canada has demonstrated that operating lighting, ventilation, and dehumidification as dispatchable loads can integrate more renewable energy [37].

A modular wastewater treatment system produced by Lifewater™ is used by many households in the Arctic to treat and safely discharge blackwater from toilets [38]. This system can improve community health and water security by reducing dependence on honey buckets and waste lagoons, which are susceptible to breaches. The water treatment power demand was analyzed on a flexible schedule, by turning on pumps, aerators, and water disinfection, coincident with wind generation. Power use data for each of these components has been modeled for this application [39].

A Water Reuse system has been developed specifically for the Arctic, which enables greywater from sinks, showers, and laundry to be reused within a household, thus reducing the need to haul water from the community washeteria [40]. The system uses pumps to treat water through various filters, reverse osmosis units, and ultraviolet and ozone disinfection systems, which can be operated flexibly. Power use data has been collected for each of these components [41].

Finally, electric water heating was also chosen as a dispatchable load. The water heater operates when excess energy is abundant and deactivates when energy output is low, such that water temperature remains within an appropriate range (~49–60 °C or ~120–140 °F). A standard 190 L (50 gallon) residential electric water heater was chosen and modeled for typical patterns of energy use based on data from the Electric Power Research Institute [42].

The average seasonal and diurnal behaviors of typical load operations for one unit of the four dispatchable loads are shown in Fig. 5. Each season is three months long, defined by fall (September through November), winter (December through February), spring (March through May), and summer (June through August). While these load profiles would deviate in practice, given that they would be dispatched to accommodate a specific situation, this analysis was based on how the modular loads operate in the status quo, as a conservative case.

The CropBox© has the highest load and is relatively consistent on a diurnal basis, aside from a few hours in which lighting is turned off. The water-based loads all have various peaks in demand when treating water, although the Lifewater™ system has the lowest load.

Since each of the 25 households would need Lifewater™, Water Reuse, and water heater systems, the analysis of each dispatchable load included 25 units. However, only one CropBox© would be installed, as it is a large load best operated at a community scale, so the analysis included only one unit. Also, though most or all housing units might already have water heaters installed, for the purpose of this dispatchability study the water heater was evaluated as if none were existing. Furthermore, combinations of different dispatchable load types were considered. It should also be noted that the costs of the new devices were not considered in this analysis. A block diagram of the electric network topology to show how the energy is being sourced and distributed to the system loads is displayed in Fig. 6.

3. Results and discussion

The capacity factor and resulting economics of each wind turbine are presented in Sections 3.1 and 3.2, respectively, and results of dispatchable load integration metrics are presented in Section 3.3.

3.1. Capacity factor

The capacity factors from operating each of the 24 selected wind turbines for two test cases—50% (assuming no dispatchable loads) and 100% (including dispatchable loads) instantaneous wind supply—were analyzed. A comparison of the capacity factors demonstrated minimal differences between 50% and 100% instantaneous wind supply scenarios (see Appendix D). This was due to the relatively high technical minimum load of the diesel generator that is needed to be maintained and the curtailment of the wind energy. The 100% wind penetration case was used for the remaining calculations since dispatchable loads were also evaluated for the community.

From the 24 wind turbines initially considered, six were selected for the community based on a criteria range of 50–5000 kW and capacity factor range of 5–40% [36]. For the selected turbines—-which included the Entegrity (65 kW), Wind Energy Solution (70 kW, 80 kW, and 100 kW), Vestas V27 (225 kW), and EWT DirectWind 52 (250 kW)—the capacity factors, wind energy absorption rate, wind energy rejection rate, and percentage of load demand covered by wind were calculated, as shown in Fig. 7. The wind energy absorption rate is the percentage of wind energy that can be absorbed by the power grid. The wind energy rejection rate is the percentage of energy rejected by the grid.

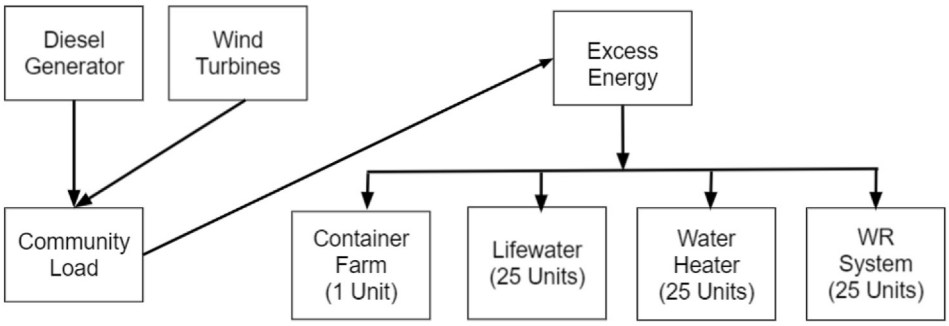

Fig. 6. Block diagram of electric network topology demonstrating generation from diesel and wind to meet the community load, then meeting dispatchable load demand (Container Farm, Lifewater, Water Heaters, Water Reuse [WR] system). Dispatchable loads are first utilized with any excess energy beyond community load.

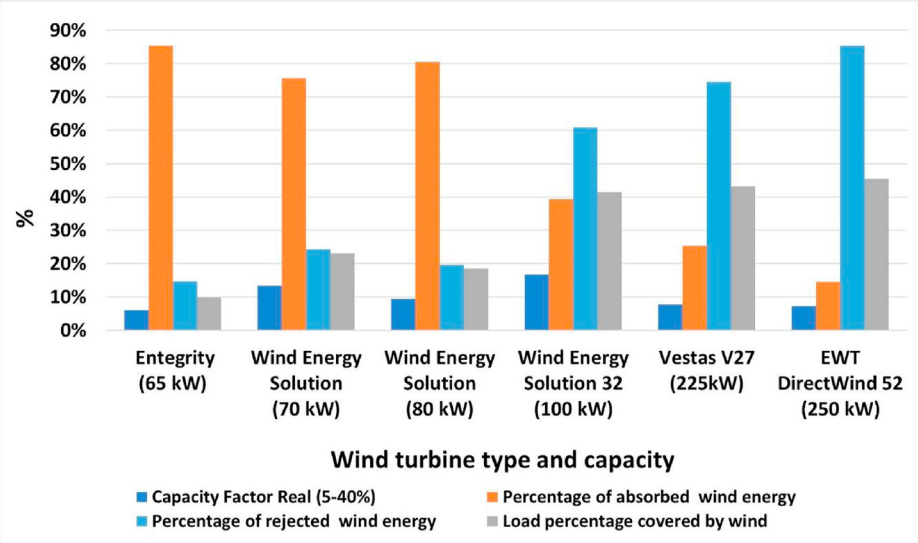

Fig. 7. Capacity factors, wind energy absorption rate, wind energy rejection rate, and wind supply rate based on the convolution of the hourly excess wind energy and load demand, not including dispatchable loads. The wind turbines selected have the capacity within the criteria range of 50–5000 kW and capacity factor range of 5–40%. Larger wind turbines were able to meet a higher percentage of the community's load but with diminishing returns above 100 kW.

The capacity factor ranged from 6.1% to 13.3% depending on the wind turbine. The absorption rate of the total generated wind energy decreased as wind turbine capacity increased. Wind turbines with rated power greater than 2.5 times of the average community load showed diminishing returns because of the significant decrease in capacity factor.

3.2. Economics

The LCOE and capacity cost of each turbine, based on their resulting capacity factors, are displayed in Fig. 8. These LCOE calculations only account for wind generation to meet the community load and do not account for any excess energy used to power dispatchable loads. Thus, this calculation is conservative given that including dispatchable loads would decrease LCOE by using more of the generation capacity of the wind turbines. The cost per installed wind capacity varied from about $27,100/kW to $16,600/kW with increasing capacity of the wind turbine, as shown in Fig. 8. In this figure, there was a decreasing trend with increasing capacity as economies of scale were realized.

Based on the economic calculations, the 100 kW Wind Energy Solution 32 wind turbine would be best suited for the community as it has the highest capacity factor of about 16.7% and a relatively low cost per installed capacity of about $20,700/kW. The turbine has a corresponding LCOE of ~$1.15/kWh. This calculated LCOE of wind energy is higher than the conventional LCOE of diesel electric generation, which is $0.92/kWh and $0.62/kWh with a subsidy [43].

However, with the inclusion of the excess wind energy absorbed by dispatchable loads, there is an increase in capacity factor and decrease in LCOE of the wind turbine. The increase in capacity factor results from utilization of otherwise wasted energy from the wind turbines by the dispatchable loads. The improvement in capacity factor and LCOE is shown in Table 3 for the case of choosing one type of dispatchable load to install in the community.

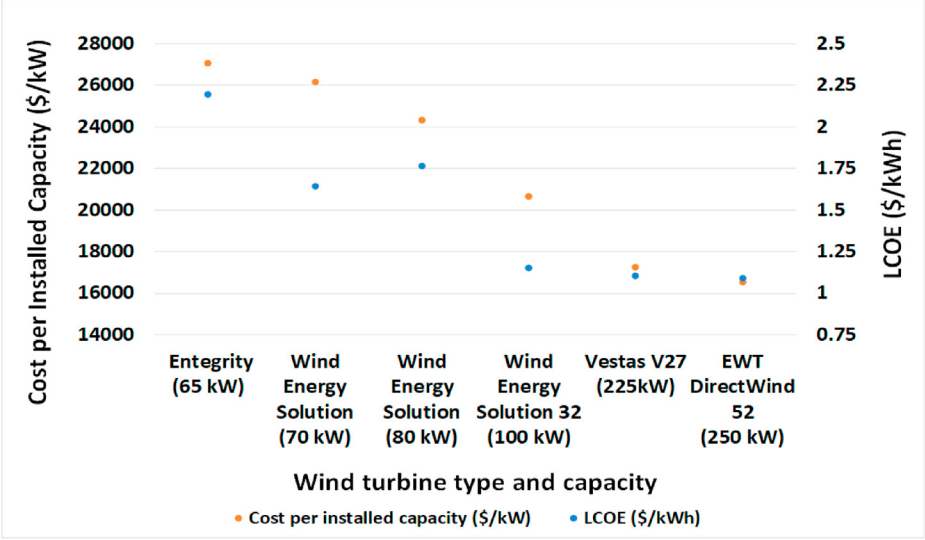

Fig. 8. Levelized cost of electricity (LCOE) and cost per installed capacity of the wind turbines selected.

Table 3
Levelized Cost of Electricity of a 100 kW Wind Energy Solution 32 wind turbine meeting demand of the community with excess wind energy utilized to power each type of dispatchable load. Water heaters provide the greatest utilization of excess wind energy in this case.

	CropBox©	Lifewater™	Water Heater	Water Reuse
Wind Turbine Capacity Factor	21.0%	18.3%	24.5%	19.2%
Wind Turbine LCOE ($/kWh)	0.96	1.07	0.85	0.84

Table 4
Annual dispatchable load demand of each load with the percentage of the total demand met by the excess energy generated by each wind turbine.

	CropBox©	Lifewater™	Water Heater	Water Reuse
Number of units	1	25	25	25
Annual Dispatched Load Demand (MWh)	58	23	120	32
Entegrity (65 kW)	9%	14%	5%	12%
Wind Energy Solution (70 kW)	21%	25%	15%	24%
Wind Energy Solution (80 kW)	15%	21%	10%	19%
Wind Energy Solution 32 (100 kW)	65%	63%	57%	67%
Vestas V27 (225 kW)	76%	75%	69%	79%
EWT DirectWind 52 (250 kW)	84%	80%	78%	86%

3.3. Dispatchable loads

In this section, the effect of incorporating dispatchable loads to absorb excess energy is discussed. First, the electric demand of each dispatchable load (discussed in Sec. 2.6), is modeled to operate on the excess generation of each wind turbine on an annual basis, using the convolution method and scenarios of dispatchable load combinations. Then, the integration of dispatchable loads with excess wind energy on an hourly basis for finer temporal-scale analysis is presented.

3.3.1. Annual integration of each dispatchable load

The dispatchable load demand was input into the convolutional process to determine the best fit between dispatchable loads and wind turbines to allow for the maximum percentage of wind penetration. The metrics used to evaluate this recommendation were the total annual amount of excess wind energy used to power each dispatchable load, expressed as total energy in kWh (named “dispatched load absorbed”) and as a percentage of the total dispatchable load demand (“dispatched load percentage”). For example, an EWT Direct Wind 52 (250 kW) turbine would generate about 938 MWh of excess energy with no dispatchable loads; however, with an installation of 25 water heaters, 93 MWh of that excess energy would be absorbed, accounting for 78% of the annual load demand of the water heaters. This result does not consider control of the water heater consumption profile. Higher dispatched load percentages mean that the dispatchable load demand can be met predominantly by what would otherwise be excess wind energy. The results of evaluating the simulations for each turbine and load, given the above metrics, are summarized as a total value for an entire year, based on the results of the convolutional process.

Table 4 displays the number of units of each dispatchable load, the annual dispatched load demand, and the percentage of the total demand that would be met by excess energy from each turbine. Higher wind capacities allow for higher amounts of the dispatchable load demand to be met, as expected. For turbines with capacities less than 100 kW, the Lifewater™ has the highest percentage of its load met; for turbines with capacities of 100 kW or more, the Water Reuse system has the highest percentage of its load met.

The total annual amount of load met in MWh is presented in Fig. 9 for each of the dispatchable load and wind turbine combinations. Of all dispatchable loads, water heaters absorb the most total excess energy, followed by the CropBox©. Both loads have a relatively constant baseload in their status quo demand profile, and thus have a high likelihood of absorbing wind energy when it is available. Water heating has especially been noted for its high potential for demand flexibility as a dispatchable load and thus may be able to shift its profile to align more closely with renewable generation, if controlled in an optimal manner in real deployment [44]. The Lifewater™ system does have a water heating component, although the component is not included in this analysis given that the heating component load data have not been collected. In practice, the Lifewater™ system may resemble some of the same characteristic results as water heaters.

3.3.2. Annual integration of combinations of dispatchable loads

The evaluation of combinations of dispatchable load types was also investigated. These combinations were chosen using any reasonable number or type of dispatchable loads, as long as the total annual dispatchable load demand was less than or equal to the available excess energy. These results are summarized over an entire year per the convolutional process, as shown in Fig. 10.

Although community preferences may dictate different combinations of loads, the scenarios in Fig. 10 are an example of several functional options. In general, the annual dispatched percentage increased significantly with an increase in wind capacity, as can be seen in the difference between the 225 kW Vestas V27 and 250 kW EWT Direct Wind 52. With an increase in wind turbine capacity of 25 kW and with the same number of dispatchable loads, there is about a 12% increase in annual dispatched percentage.

3.3.3. Diurnal integration of each dispatchable load

As opposed to considering the dispatchable load demand as an aggregate amount of energy over a year, the coincidence of the demand profile with excess wind energy supply can be analyzed over each hour. In other words, how does dispatchable load demand align with excess wind generation on an hourly basis over an average day? All turbines were analyzed; however, given similar results among turbines, only the 100 kW Wind Energy Solution 32 turbine is presented. The generation per turbine at an hourly resolution is shown for an average day in each season in Fig. 11.

The output of excess wind energy from the turbine is highest at night and in the spring. The ratio of this excess wind energy compared to the demand of each dispatchable load, or dispatched percentage, was calculated for each hour of the year and averaged to display a typical day in each season, as shown in Fig. 12.

On average, there is sufficient excess wind to power the dispatchable loads, as the dispatched percentage (ratio of excess wind to dispatchable load) is greater than 100%. The Water Reuse and

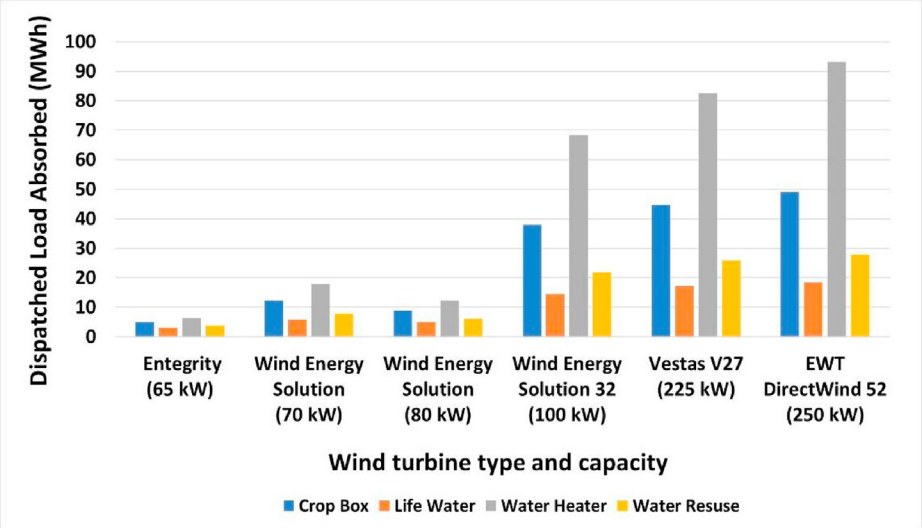

Fig. 9. Annual dispatchable load demand absorbed by excess wind energy output (MWh) demand of simulating 25 Lifewater™ units, 25 Water Reuse systems, 25 water heaters, or 1 CropBox© paired with each wind turbine considered. From the results in this figure, the water heater is best able to absorb excess energy.

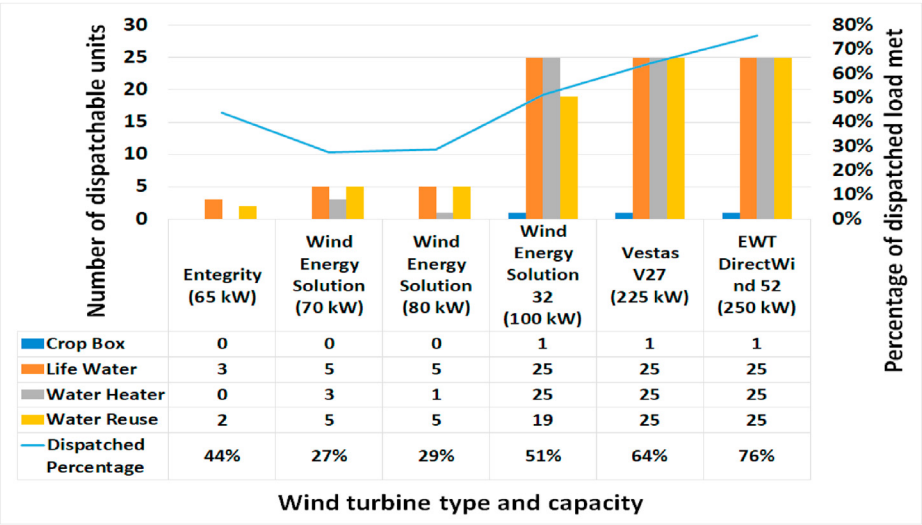

	Entegrity (65 kW)	Wind Energy Solution (70 kW)	Wind Energy Solution (80 kW)	Wind Energy Solution 32 (100 kW)	Vestas V27 (225 kW)	EWT DirectWind 52 (250 kW)
Crop Box	0	0	0	1	1	1
Life Water	3	5	5	25	25	25
Water Heater	0	3	1	25	25	25
Water Reuse	2	5	5	19	25	25
Dispatched Percentage	44%	27%	29%	51%	64%	76%

Fig. 10. Dispatchable load units and annual dispatched load percentage for combinations of dispatchable loads with increasing installed capacity.

Lifewater™ systems have the highest ratio, given their low power usage during most of the day aside from peak power events. Across all loads, excess wind has the most difficult time meeting dispatchable load demand during midday in the summer.

In Fig. 12, averages over the course of each hour of the day are shown for each dispatchable load as one average day per season. However, when analyzing each hour of an entire year, not averaged by season, there are several hours in which excess wind cannot meet dispatchable load demand, as shown in Table 5. In practice, the dispatchable load profiles would be tailored to turn off in hours when no wind is available. These results are intentionally conservative, only integrating the loads using typical demand profiles (no load control). The Lifewater™ systems have the fewest hours in which load is not met, partly due to the lower system capacity (~500 W).

While Fig. 12 suggests there is enough excess wind power to meet demand on average, an hourly analysis of real (not averaged) data demonstrates there is frequently an insufficient amount of excess wind energy. The Lifewater™ system is best suited for absorbing excess power from the 100 kW Wind Energy Solution 32 wind turbine, which may be because it has one of the most consistent and lowest load profiles. However, given the Lifewater™ system has the lowest overall electricity demand, it used the least amount of excess wind energy available compared to the other dispatchable loads.

If dispatchable load types and their demand profiles were optimized, the total demand profile met would most likely be higher in magnitude with less operation during times of low wind energy output. For example, the water heater has a relatively high power demand when heating water, with substantial energy use over a year and considerable potential for energy storage. Thus, if the water heater operations were optimized, it could store sufficient excess wind energy in the form of heated water to bridge periods of low wind generation, with minimal effect on consumer demand. Although the percentage of total annual dispatchable load demand met by excess wind energy is lower for water heaters than other loads in this study, future study may demonstrate they can absorb more excess energy when optimized.

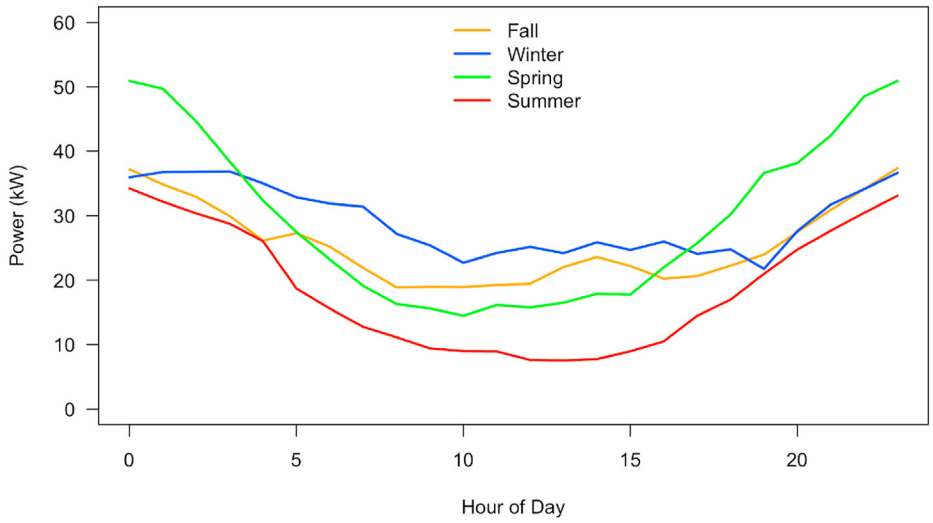

Fig. 11. Excess wind power from the 100 kW Wind Energy Solution 32 wind turbine averaged diurnally for each season. Wind generation is lowest in the summer and highest during spring nights and midday winter times.

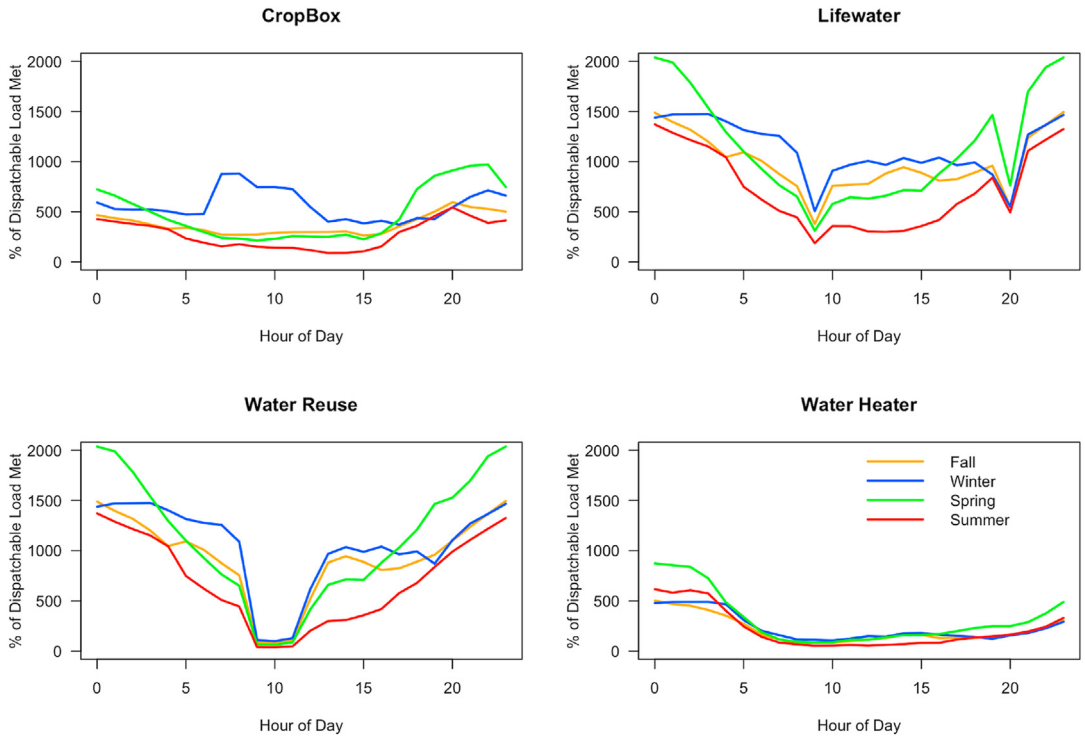

Fig. 12. Hourly and seasonal percent of each dispatchable load met by excess wind power generation from the 100 kW Wind Energy Solution 32 wind turbine.

Table 5
Capability of excess wind power or energy? Generated by the 100 kW Wind Energy Solution 32 wind turbine to meet the demand of dispatchable loads.

Dispatchable Load	CropBox©	Lifewater™	Water Reuse	Water Heater
Percentage of year in which excess wind meets dispatchable load demand	58%	64%	61%	51%
Percentage of total annual dispatchable load demand met by excess wind	63%	65%	51%	55%

4. Conclusion

The goal of this study was to develop an alternative wind resource assessment method using a rural Arctic community's airport meteorological data and to determine the best wind turbine for installation based on total generation and ability to match excess generation with specific dispatchable loads. Given the highest capacity factor of 16.7% and LCOE of $1.15/kWh, a 100 kW Wind Energy Solution 32 wind turbine was determined to be best suited for the community.

Furthermore, several types of dispatchable loads—a CropBox©, Lifewater™ system, Water Reuse system, and water heater—were analyzed to integrate with coincident excess energy generation, while also providing FEW security benefits to the community. The convolution of the hourly excess energy from wind turbine generation and hourly load demand of each dispatchable load resulted in different absorption rate scenarios; ultimately, the Lifewater™ system provided the optimal match based on the ratio of its demand to excess wind energy available. Based on integration with all potential wind turbines, the Water Reuse system offered the highest annual dispatched percentage, at about 86%, with the largest 250 kW EWT DirectWind 52 (250 kW) wind turbine.

Excess wind energy was most inadequate at meeting dispatchable load demand during midday and summertime periods. While calculation of annual dispatchability percentages showed that dispatchable loads can handle the intermittency of the wind resources, it must be taken into consideration that this study used 1-h resolution datasets, which evened out fluctuations that occur at higher resolutions. One consequence of this approach is that the excess energy would not be evenly distributed over an hour and thus might not be able to be used as calculated. However, there is sufficient flexibility in the dispatchable load capacity to be able to accommodate fluctuations due to intermittency of excess wind power generation.

Nevertheless, in future work, the capacity factor and cost analyses can be improved by the inclusion of the actual operating schedule of each diesel generator instead of using the average generator capacity. Inclusion of the actual run schedule will greatly improve the capacity factor since the technical minimum is more accurate and lower, which in turn will decrease the LCOE. Dispatchable load scenarios can be refined by collaborating with the communities to understand their preferences of wind turbines, dispatchable load choices, and number of preferred and useable dispatchable load units. Furthermore, the dispatchable load integration model should include modeling optimal control of dispatchable loads and at higher temporal resolution. More work is also needed to understand the impact of integrating dispatchable loads into the grid in practice along with the scheduling of those loads.

This research forms a foundation for the use of alternative wind resource assessment methods, wind turbine selection procedures, and potential dispatchable load installations in rural Arctic communities. Ultimately, co-deployment of wind turbines and dispatchable loads could improve the community's food, energy, and water security while reducing their reliance on fossil fuels. Although this study focused on a rural Alaska community, the tool developed can be utilized to assess any rural community with similar conditions throughout the developing world. The climates will vary but the tool can be set up for different wind turbines and input data. The issues of food, energy, and water security in off-grid communities are not only applicable in Alaska; similar conditions exist throughout the developing world.

CRediT authorship contribution statement

Chong Her: Conceptualization, Methodology, Validation, Formal analysis, Investigation, Data curation, Writing – original draft. **Daniel J. Sambor:** Conceptualization, Methodology, Validation, Formal analysis, Investigation, Data curation, Writing – original draft, Writing – review & editing. **Erin Whitney:** Conceptualization, Resources, Writing – review & editing, Supervision, Project administration, Funding acquisition. **Richard Wies:** Conceptualization, Methodology, Writing – review & editing, Supervision.

Declaration of competing interest

The authors declare that they have no known competing financial interests or personal relationships that could have appeared to influence the work reported in this paper.

Acknowledgements

Funding: The work described in this paper was funded by the United States National Science Foundation, Award No. 1740075: INFEWS/T3: “Coupling Infrastructure Improvements to Food-Energy-Water System Dynamics in Small Cold Region Communities: MicroFEWs.”

Chong Her completed this analysis with his co-authors as part of his Masters thesis at the Institute of Engineering, Hanze University of Applied Sciences, Zernikeplein 11, 9747 AS Groningen, Netherlands. The authors of this paper would like to express their gratitude and sincere appreciation to Jeremy VanderMeer, Rich Stromberg, Michele Chamberlain, Henry Huntington, and Joe Selmont for their valuable comments, suggestions, and proofreading of this research paper.

Appendix A. Wind assessment equations are as follows

The data were analyzed to determine the wind resource characteristics in each community and provide a useful summary of the validated wind resource data. This summary included the mean wind speed, annual mean wind speed, standard deviation, turbulence intensity, Weibull distribution, histogram, wind power density, and wind rose.

The mean wind speed (V_{ave}) is a simple average of all the values throughout the period of interest:

$$V_{ave} = \frac{1}{N_{valid}} \sum_{i=1}^{N_{valid}} V_i \qquad \text{Eq. A.1}$$

where V_i is the wind speed in the time series and N_{valid} is the number of valid data points. This means wind speed can be a misleading indicator of the wind resource as it may not reflect a full seasonal cycle of wind variations and could be biased from measurement periods less than a year, large gaps in the data log, and non-integer numbers of years recorded. This bias could mean that some months may be favored or represented more often [22].

The annual mean wind speed ($V_{an_{ave}}$(m/s)) is calculated by taking the mean of each calendar month's average wind speed:

$$V_{an_{ave}} = \frac{1}{12} \sum_{i=1}^{12} V_{m_{ave},i} \qquad \text{Eq. A.2}$$

where $V_{m_{ave},i}$ is the monthly mean wind speed. This method helps reduce the data bias and is a more accurate representation of the wind resource, but data of at least 12 months is needed [22].

To calculate the wind power density from the wind resource, it is necessary to evaluate the wind speed frequency distribution. The speed frequency distribution is the number of occurrences of a wind speed within a bin width, typically 0.5 m/s or 1 m/s [22]. Here, we use 1 m/s and a Weibull distribution. The Weibull distribution has been found to be a best-fit approximation of the speed frequency distribution for wind assessment [23,24]. The Weibull distribution function considers the specific wind velocity (V(m/s)), shape factor (k), and scale factor (c(m/s)) [25]:

$$f(V) = \frac{k}{c} * \left(\frac{V}{c}\right)^{k-1} * e^{-\left(\frac{v}{c}\right)^k} \qquad \text{Eq. A.3}$$

The Weibull parameters can be calculated as follows:

$$k = \left(\frac{\sigma}{V_{an_{ave}}}\right)^{-1.086} \quad \text{Eq. A.4}$$

$$c = \frac{V_{an_{ave}}}{\Gamma\left(1+\frac{1}{k}\right)} = 1.1 * V_{an_{ave}} \quad \text{Eq. A.5}$$

where σ (m/s) is the annual standard deviation of the wind speed, $V_{an_{ave}}$(m/s) is the annual average wind velocity, and Γ is the gamma function given by:

$$\Gamma(x) = \int_0^\infty t^{x-1} e^{-t} dt \quad \text{Eq. A.6}$$

The heights of the wind speeds measured from the meteorological stations are 10 m for all communities in this study. The most common vertical wind profile extrapolation method is the power-law [23,26]:

$$V_{z2} = V_{z1} * \left(\frac{z2}{z1}\right)^m \quad \text{Eq. A.7}$$

where m is the power-law exponent of the wind speed and is also known as the roughness or friction coefficient, which is highly dependent on the roughness of the terrain. A table of m values is shown in Table A1 [23,27].

Table A.1
Roughness coefficient for different terrain types

Roughness Coefficient (m)	Terrain Type
0.13	Water Area
0.16	Shore
0.20	Plain
0.24	Wood Plain
0.30	City

The power of the wind can be calculated using the following equation, where ρ (kg/m^2) is the air density and A (m^2) is the rotor swept area [25]:

$$P(V) = \frac{1}{2} * \rho * A * V^3 \quad \text{Eq. A.8}$$

The air density is temperature-dependent and can be calculated using air pressure (converted to N/m^2 = 1 Pa where standard atmospheric pressure is 101,325 Pa absolute) and air temperature (converted to Kelvin, or K) readings from the meteorological station. The average air density of a specific location can be calculated as:

$$\rho = \frac{p}{R * T} \quad \text{Eq. A.9}$$

where p (N/m^2) is the air pressure, T(K) is the air temperature, and R is the universal gas constant (about 287 J/kg*K).

From the Weibull distribution calculated in Equation (A.3), the wind power density (P) can be calculated using Equation (A.10):

$$P = \frac{1}{2} * \rho * V^3 * f(prob) \quad \text{Eq. A.10}$$

$$f(prob) = f(V) * 0.5 \quad \text{Eq. A.11}$$

where $f(V)$ is the Weibull probability density function with a bin width of 1 m/s.

Appendix B. List of wind turbines considered

Table B.1
Overall, 24 wind turbines were considered based on already installed and test cases in Alaska [28–31].

Performance	Diameter	Tower height	Rated Power	Annual Power production @">@ 4 m/s	Cut-in wind speed	Rated wind speed	Cut-out wind speed	Operation temperature
Eocycle (EO25)	16 m	23.8 m	25 Kw	40 MWh	2.75 m/s	11 m/s	20 m/s	
Energie PGE	11 m	18 m	35 kW	19.527 MWh	4.8 m/s	14 m/s	25 m/s	–
Entegrity	15 m	25 m	65 kW	87 MWh	4.6 m/s	17 m/s	22.4 m/s	−40C
Wind Energy Solution	20.3 m	15, 18, 24, 30 m	50 Kw	124 MWh	<3 m/s	9.5 m/s	25 m/s	−20 °C up to +40 °C
Wind Energy Solution	17.9 m	18, 24, 30, 39 m	80 kW	74 MWh	<3 m/s	13 m/s	25 m/s	−20 °C up to +40 °C
Aeolos H	24.5 m	30 m	100 kW	100 MWh	2.5 m/s	10 m/s	None	−20 °C up to +50 °C
Northern Power Systems	20.9 m	35.7 m	100 kW	77 MWh	3.5 m/s	15.0 m/s	25 m/s	−40 °C up to +50 °C
Wind Energy Solution 32	32 m	30, 39, 48 m	100 kW	207 MWh	2 m/s	9 m/s	16 m/s	−20 °C up to +40 °C
XANT M-21	21 m	23, 38 m	100 kW	–	3.5 m/s	11 m/s	20 m/s	–
XANT M-24	24 m	23, 38 m	100 kW	–	3 m/s	10 m/s	20 m/s	–
Vestas V27	27 m	110 m	225 kW	–	3 m/s	15 m/s	25 m/s	–
EWT DirectWind 52	52 m	35, 40 and 50 m	250 kW	.	3 m/s	10 m/s	25 m/s	–
Wind Energy Solution	30 m	30, 39, 48 m	250 kW	207 MWh	<3 m/s	13 m/s	25 m/s	−20 °C up to +40 °C
EWT DirectWind 52	52 m	35, 40 and 50 m	500 kW	1750 MWh	3 m/s	10 m/s	25 m/s	–
EWT DirectWind 54	54 m	40, 50 and 75 m	500 kW	1550 MWh	2.5 m/s	10 m/s	25 m/s	–
EWT DirectWind 61	61 m	46 and 69 m	500 kW	1550 MWh	2.5 m/s	11.5 m/s	25 m/s	–
Vestas V39	39 m	40.5 and 53 m	500 kW	–	4 m/s	15 m/s	25 m/s	−30C to +40C
EWT DirectWind 61	61 m	46 and 69 m	750 kW	1550 MWh	2.5 m/s	11.5 m/s	25 m/s	–
EWT DirectWind 52	52 m	35, 40 and 50 m	900 kW	1750 MWh	3 m/s	14 m/s	25 m/s	–
EWT DirectWind 54	54 m	40, 50 and 75 m	900 kW	1550 MWh	2.5 m/s	14 m/s	25 m/s	–
EWT DirectWind 61	61 m	46 and 69 m	900 kW	1550 MWh	2.5 m/s	11.5 m/s	25 m/s	–

Appendix C. Cost per installed capacity and LCOE tables and values

Table C.1
Project costs and total cost per installed capacity [36].

Installed wind capacity (kW)	Analysis and design (k$">$/kW)	Hardware and transport (k$">$/kW)	Balance of system (k$">$/kW)	Total (k$">$/kW)
50	3.805	10.661	15.353	29.819
100	2.284	8.251	10.145	20.680
500	0.715	4.552	4.438	9.705
1000	0.439	3.523	3.357	7.319
2000	0.273	2.728	2.676	5.676
5000	0.148	1.945	2.143	4.236

Table C.2
Values of LCOE of different installed capacity and capacity factor [36].

Installed wind capacity (kW)	5% average capacity factor ($">$/kWh)	10% average capacity factor ($">$/kWh)	20% average capacity factor ($">$/kWh)	30% average capacity factor ($">$/kWh)	40% average capacity factor ($">$/kWh)
50	2.50	2.08	1.41	0.96	0.73
100	1.79	1.48	0.99	0.67	0.52
200	1.25	1.04	0.71	0.49	0.38
500	0.87	0.72	0.49	0.34	0.27
1000	0.64	0.54	0.38	0.27	0.21
2000	0.48	0.41	0.30	0.22	0.17
5000	0.42	0.35	0.24	0.17	0.14

Appendix D. Capacity factors of operating 24 specific wind turbines for two cases—50% (no dispatchable loads) and 100% instantaneous wind supply

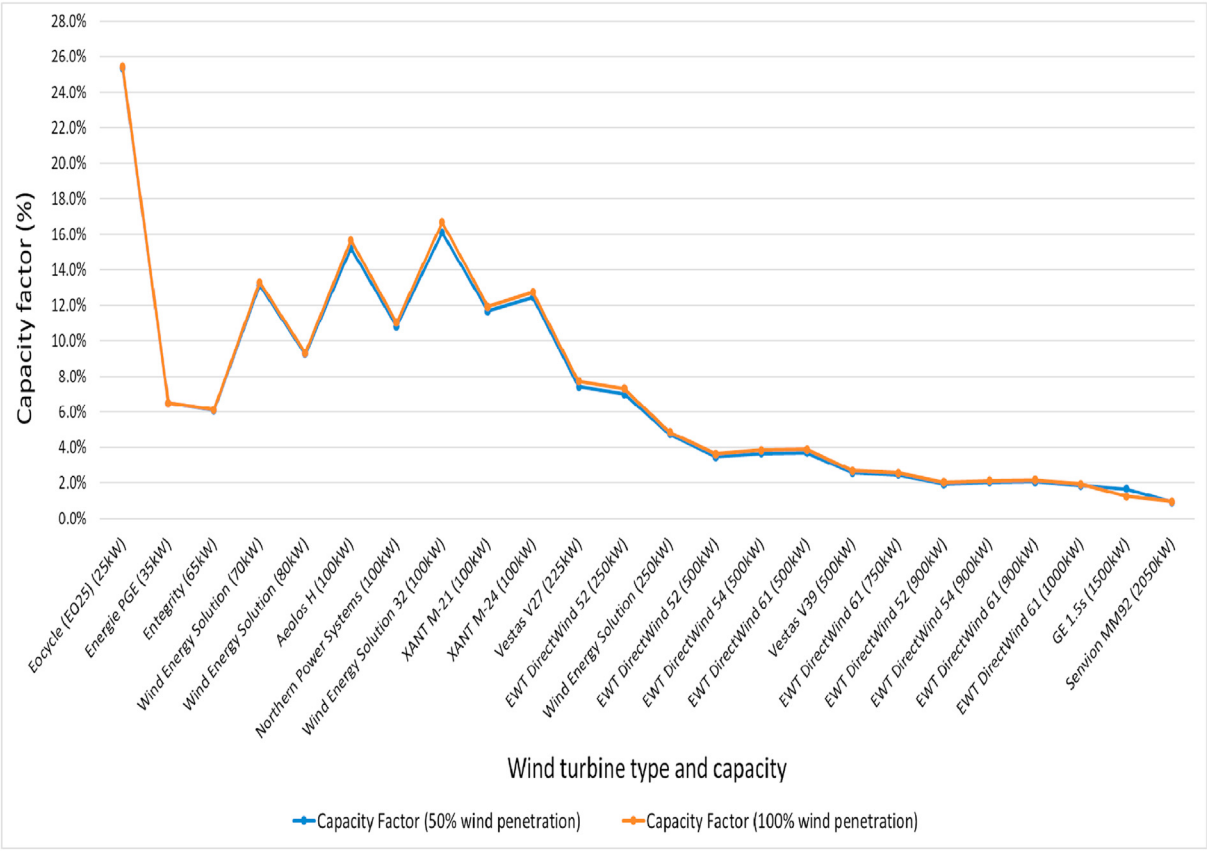

Fig. D.1. Comparison of the capacity factors of 50% and 100% instantaneous wind supply scenarios for the 24 wind turbines.

References

[1] Y. Hossain, P.A. Loring, T. Marsik, Defining energy security in the rural north—historical and contemporary perspectives from Alaska, Energy Research & Social Science 16 (2016) 89–97, https://doi.org/10.1016/j.erss.2016.03.014.

[2] W. Isherwood, J.R. Smith, S.M. Aceves, G. Berry, W. Clark, R. Johnson, R. Seifert, Remote power systems with advanced storage technologies for Alaskan villages, Energy 25 (10) (2000) 1005–1020, https://doi.org/10.1016/s0360-5442(00)00028-1, 2000.

[3] C. Lawrence, D.M. Hamilton, R.B. White, G.M. Lammers, Population, climate, and electricity use in the Arctic integrated analysis of Alaska community data, Popul. Environ. (2011) 1–15, https://doi.org/10.1007/s11111-011-0145-1, 2011.

[4] Alaska Energy Authority, Power cost equalization program, statistical data by community, amended, authority Alaska energy, anchorage, AK. https://data-aideaaea-soa.hub.arcgis.com/datasets/857181186b164d26b667e5d1c954da3c_0/data?orderBy=ResRate&orderByAsc=false, 2019. (Accessed 10 April 2020).

[5] S.C. Gerlach, C. Loring, P.A. Loring, A. Turner, D.E. Atkinson, Food systems, environmental change, and community needs in rural Alaska, in: A.L.L. Hajo Eicken (Ed.), North by 2020: Perspectives on a Changing North, University of Alaska Press, Fairbanks, AK, 2011, 2011.

[6] D.V. Fazzino, P.A. Loring, From crisis to cumulative effects: food security challenges in Alaska, 2009, NAPA Bull 32 (2009) 152–177, https://doi.org/10.1111/j.1556-4797.2009.01033.x.

[7] S.C. Gerlach, P.A. Loring, A. Turner, D.E. Atkinson, Food systems, climate change, and community needs, in: A.L. Lovecraft, H. Eicken (Eds.), North by 2020, University of Alaska Press, Fairbanks, 2011, pp. 111–134.

[8] J. Coello, R. Escobar, C. Dávila, G. Villanueva, J. Chiroque, Micro hydro power plants and other alternative energies: contributions of Practical Action – ITDG to rural development, in: Environmental Cases Studies and White/Technical Papers, Port of Entry, the Environmental Business Network for the Americas, 2006.

[9] N.B. Chang, Md Hossain, A. Valencia, J. Qiu, Q. Zheng, L. Gu, M. Chen, J.W. Lu, A. Pires, C. Kaandorp, E. Abraham, M.c. Ten Veldhuis, N. van de Giesen, B. Molle, S. Tomas, N. Mouheb, D. Dotta, R. Declercq, M. Perrin, G. Molle, Integrative technology hubs for urban food-energy-water nexuses and cost-benefit-risk tradeoffs (II): design strategies for urban sustainability, Crit. Rev. Environ. Sci. Technol. (2020) 1–51, https://doi.org/10.1080/10643389.2020.1761088.

[10] M. Ranaboldo, L. Ferrer-Martí, E. Velo, Micro-scale wind resources assessment for off-grid electrification projects in rural communities. A case study in Peru, Int. J. Green Energy 11 (1) (2014) 75–90, https://doi.org/10.1080/15435075.2013.769878.

[11] S. Rehman, T.O. Halawani, Statistical characteristics of wind in Saudi Arabia, Renew. Energy 4 (8) (1994) 949–956.

[12] S. Rehman, I.M. El-Amin, F. Ahmad, S.M. Shaahid, A.M. Al-Shehri, J.M. Bakhashwain, Wind power resource assessment for Rafha, Saudi Arabia, Renew. Sustain. Energy Rev. 11 (5) (2007) 937–950.

[13] United Nations Environment Programme UNEP, SWERA, solar and wind energy resource assessment. http://en.openei.org/apps/SWERA/, 2006. (Accessed 27 March 2020).

[14] United States Census Bureau, American community survey 5-year estimates. https://www.census.gov/en.html, 2014-2018. (Accessed 1 October 2020).

[15] University of Alaska, MicroFews, Website, http://ine.uaf.edu/microfews. (Accessed 15 March 2020).

[16] E. Whitney, W.E. Schnabel, S. Aggarwal, D. Huang, R.W. Wies, J. Karenzi, A.D. Dotson, MicroFEWs: a food–energy–water systems approach to renewable energy decisions in islanded microgrid communities in rural Alaska, Environ. Eng. Sci. 36 (2019), https://doi.org/10.1089/ees.2019.0055.

[17] H. Babaie, A. Davarpanah, N. Dhakal, Projecting pathways to food–energy–-water systems sustainability through ontology, Environ. Eng. Sci. 36 (2019) 808–819, https://doi.org/10.1089/ees.2018.0551.

[18] X. Cai, K. Wallington, M. Shafiee-Jood, L. Marston, Understanding and managing the food-energy-water nexus – opportunities for water resources research, Adv. Water Resour. 111 (2018) 259–273, https://doi.org/10.1016/j.advwatres.2017.11.014.

[19] Iowa State University, Iowa environmental Mesonet: ASOS network, Website: https://mesonet.agron.iastate.edu/request/download.phtml?network=AK_ASOS, , 2001. (Accessed 20 April 2020).

[20] Darly, H., iem_scraper_example.py, GitHub, Website: https://github.com/akrherz/iem/blob/master/scripts/asos/iem_scraper_example.py, Accessed on 7 June 2020.

[21] B.H. Bailey, S.L. McDonald, D.W. Bernadett, M.J. Markus, K.V. Elsholz, in: Wind Resources Assessment Handbook, National Renewable Energy Laboratory (NREL). AWS Scientific, Inc., 1997. Subcontract No. TAT-5-15283-01. Website: https://www.nrel.gov/docs/legosti/fy97/22223.pdf. (Accessed 10 March 2020).

[22] J. Bouget, M. Brower, M. Eberhard, M. Filippelli, M. Markus, in: Wind Resources Measurement: Guidelines for Islands, International Renewable Energy Agency, 2015. https://www.irena.org/-/media/Files/IRENA/Agency/Publication/2015/IRENA_Island_Wind_Measurement_2015.ashx. (Accessed 10 March 2020).

[23] L. Tenghiri, Y. Khalil, F. Abdi, A. Bentamy, Potential assessment of hybrid pv-wind systems for household applications in rural areas: case study of Morocco, E3s Web of Conferences 122 (2019), https://doi.org/10.1051/e3sconf/201912202001.

[24] A.K. Azad, M.G. Rasul, M.M. Alam, S.M. Ameer Uddin, S.K. Mondal, Analysis of wind energy conversion system using Weibull distribution 90, Procedia Eng., 2014.

[25] S. Farhan Khahro, K. Tabbassum, A.M. Soomro, L. Dong, X. Liao, Evaluation of wind power production prospective and Weibull parameter estimation methods for Babaurband, Sindh Pakistan, Energy Convers. Manag. 78 (2013).

[26] B. Safari, J. Gasore, A statistical investigation of wind characteristics and wind energy potential based on the Weibull and Rayleigh models in Rwanda 35, Renewable Energy, 2010.

[27] C.G. Justus, Winds and Wind System Performance, Franklin Institute Press, Philadelphia, 1978.

[28] Alaska Energy Authority, The great state of Alaska, Website: http://www.akenergyauthority.org/What-We-Do/Energy-Technology-Programs/Wind/Resources, , 2020. (Accessed 3 July 2020).

[29] L.L.C. V3 Energy. https://www.v3energy.com/about/, 2020. (Accessed 10 August 2020).

[30] C. Pike, Nathan Green, Alaska center for energy and power, Website: http://acep.uaf.edu/media/288911/Smyth-Pike-Whitney_Eocycle_Kotzebue_Final.pdf, , 2017. (Accessed 18 June 2020).

[31] T. Smyth, C. Pike, E. Whitney, Testing of the eocycle EO 25/12 tilt-up wind turbine in kotzebue, Alaska (2018). Website, http://acep.uaf.edu/media/288911/Smyth-Pike-Whitney_Eocycle_Kotzebue_Final.pdf. (Accessed 15 June 2020).

[32] Wind-turbine-model. https://www.wind-turbine-models.com/manufacturers, 2020. (Accessed 10 August 2020).

[33] Aeolos Wind Turbine, Aeolos wind turbine 100kW, Website, http://www.windturbinestar.com/100kwh-aeolos-wind-turbine.html, 2020. (Accessed 15 May 2020).

[34] Wind Energy Solution, WES 250, Website, https://windenergysolutions.nl/turbines/windturbine-wes-250/, 2020. (Accessed 15 May 2020).

[35] G. Caralis, K. Rados, A. Zervos, The effect of spatial dispersion of wind power plants on the curtailment of wind power in the Greek power supply system, Wind Energy 13 (2010) 339–355.

[36] J. VanderMeer, M.S. Mueller, E. Whitney, Wind power project size and component costs: an Alaska case study, J. Renew. Sustain. Energy 9 (2017), 061703, 2017.

[37] D.J. Sambor, M. Wilber, E. Whitney, M.Z. Jacobson, Development of a tool for optimizing solar and battery storage for container farming in a remote arctic microgrid, Energies *19961073* (19) (2020) 13.

[38] Lifewater engineering company. http://lifewaterengineering.com/residential/, 2020. (Accessed 10 September 2020).

[39] Rashedin, M. Lifewater Engineering Company, Website: http://lifewaterengineering.com/residential/, Accessed on 10 September 2020. 'Personal Communication'.

[40] K.A. Hickel, T.K. Thomas, M. Heavener, J.A. Warren, A. Dotson, J. Hebert, The search for an alternative to piped water and sewer systems in the Alaskan arctic, Environ. Sci. Pollut. Control Ser. 1–8 (2017) 1–8, https://doi.org/10.1007/s11356-017-8815-x.

[41] A.D. Dotson, M. Cenek, G. Michaelson, Open-source IoT framework for mobile household water Reuse system, in: 2019 IEEE Global Humanitarian Technology Conference, GHTC), Seattle, WA, USA, 2019, pp. 1–5, https://doi.org/10.1109/GHTC46095.2019.9033080, 2019.

[42] Electric Power Research Institute, Load shape library 7.0, Website: https://loadshape.epri.com/, , 2020. (Accessed 20 September 2020).

[43] Alaska Energy Authority, Power cost equalization statistical report FY19, Website: https://data-aideaaea-soa.hub.arcgis.com/datasets/857181186b164d26b667e5d1c954da3c_0/data?geometry=-160.251%2C59.390%2C-151.907%2C60.35, , 2020. (Accessed 10 November 2020).

[44] S.A. Pourmousavi, M.H. Nehrir, S.N. Patrick, Real-time demand response through aggregate electric water heaters for load shifting and balancing wind generation, IEEE Transactions on Smart Grid 5 (2) (2014) 769–778, https://doi.org/10.1109/TSG.2013.2290084.